Transforming nonisostructural wurtzite (ZnO) and rocksalt (MgO) II-VI compounds into stable alloy: The case of MgZnO

Ali Zaoui, M. Ferhat

Version of Record: https://www.sciencedirect.com/science/article/pii/S0749603620304924
Manuscript_ebcad1153eb35264a68e659b2087bfbb

Transforming nonisostructural wurtzite (ZnO) and rocksalt (MgO) II-VI compounds into stable alloy: The case of MgZnO

A. Zaoui[1,*] and M. Ferhat[2]

[1]*Univ. Lille, ULR 4515, Laboratoire de Génie Civil et géo-Environnement (LGCgE), Lille, F- 59000, France*

[2]*Département de Génie Physique, (LPMF). Université des Sciences et de la Technologie d'Oran, Mohamed Boudiaf. Oran, Algeria.*

ABSTRACT

Structural disparity between fourfold-coordinated wurtzite ZnO and sixfold-coordinated rocksalt MgO II-VI semiconductors compounds disfavor their binding into a stable II-VI alloy. Here we search for a stable Zn-Mg-O system under ambient conditions by first-principles evolutionary searches. A new thermodynamically stable cubic phase Mg_3ZnO_4, space group *P*m3m has been uncovered. Computed elastic constants, and phonon spectrum reveal the mechanic and dynamic stabilities of this phase. Using state-of-the-art quasiparticle-LDA-1/2 approach, we found a marked band-gap bowing parameter of ~4.2eV. The origin of the nonlinearity of the band gap emerges predominantly from electronic-charge-exchange effect.

Keywords: *MgZnO alloy; high-throughput computations; density functional theory (DFT); thermodynamic stability, mechanical, dynamical and electronic properties; Band-gap bowing parameter.*

*Email address: azaoui@polytech-lille.fr

ZnO and MgO are compounds of the groups II and IV of the Periodic Table. They have contrasting properties, as the former adopt the fourfold-coordinated hexagonal *B*4 wurtzite (WZ) structure ($P6_3mc$), MgO prefers the cubic sixfold-coordinated *B*1 rocksalt (RS) phase ($Fm\text{-}3m$). Moreover these nonisotructural materials are wide-band-gap semiconductors, but with a quite marked different band-gaps energies, E_g~3.37 eV for ZnO and E_g~7.6 eV for MgO at room temperature. When alloying MgO and ZnO, the direct band-gap could cover extremely short wavelength regions (deep ultraviolet (UV) spectral region). Therefore the ternary alloys MgZnO may open the route for optoelectronic device applications, such as UV detectors and UV light emitting diodes (LEDs). Nevertheless, while MgZnO have been studied over two decades, these efforts have been –unfortunately- so far impeded by a long-faced challenge related to the preparation of MgZnO alloys. Albeit that atomic size of Mg and Zn are similar, phase segregation is unpreventable. First experimental observations point out that for Mg composition from x = 0 to 0.33[1] the alloy is soluble and espouse a single wurtzite hexagonal phase. As a huge progress forward, Ishihara et al.[2] synthesized a WZ-$Mg_{0.69}Zn_{0.31}O$ alloy. Metastable cubic phase emerges at large Mg composition range for x = 0.5 to 0.86[3]. In the theoretical side, there have been great interest in the study of MgZnO alloys with wurtzite and/or rocksalt structures [4-20]; whereas few of them addressed the thermodynamic stabilities of MgO-ZnO system. Moreover, it has been shown that WZ MgZnO alloys are stable with respect to the RS-phase alloys for x<0.33[13], x<0.375[4], x<0.34[11], and x<0.67[5].

These theoretical predictions are irrelevant if the presumed phase (WZ or RS) of the alloy is not overall stable (GS) (inter alia thermodynamic stability, mechanical stability and more importantly dynamic stability). Some examples include new compounds that are in fact dynamically instable in their proposed structure, such as PtC [21], PtN [22-23], and zinc-blend (ZB) as well as ferro-magnets [24]. The argument of stability via the traditional total static energy calculations versus volume could no longer help, because it do not assure stability. More precisely, it may miss unsuspected, yet more stable phases, and/or the predicted phase is unphysical and does not exist at all, because of its dynamic instability. Albeit mechanical stability (MS) provides a necessary condition for GS, but not a sufficient one, since MS evinces only a local stability. Dynamic studies offer conclusive knowledge about global phase stability. Thereby the absence enquire of global stability of the many proposed thermodynamically stable WZ and/or RS ordered phases of MgZnO alloys poses

appealing questions: Are these "suspects" phases globally stable? Or if not and more fundamentally can we find global stable phases of MgZnO alloys?

Here, we explore possible global stability of ordered phases of MgZnO alloys, which has hitherto received limited attention, using *ab initio* evolutionary algorithm. We identify new phase of MgZnO alloys and further conduct a systematic theoretical study of electronic structure, mechanical and vibrational properties of MgO-ZnO system.

The search for the most stable and low-enthalpy structures of MgZnO alloy, was achieved using evolutionary algorithm approach as implemented in the Material project database [25-26], which has been targeted to find the most stable phase for a given chemical composition range. Total-energy calculations were performed using the density functional theory (DFT) [27] as implemented in the Quantum ESPRESSO plane-wave code [28]. The exchange-correlation functional within the linearized-gradient approximation (LDA) [29] was used. The projector-augmented wave pseudopotential method (PAW) [30] was used to represent the ion-electron interaction, with cutoff energies of 60Ry and 600Ry for the wave functions and the charge density respectively. The Brillouin zone was sampled with a 10×10×10 *k*-points mesh generated via the Monkhorst-Pack [MP] method [31] for the Mg_3ZnO_4 phase. The phonon properties are calculated using the density functional perturbation theory (DFTP) [32]. A 4×4×4 *q*-points MP mesh has been used to perform inverse Fourier transformation for Mg_3ZnO_4. These settings ensure convergence of self-consistent total energy to within 0.1meV per atom. Structure relaxation proceeded until net forces on atoms were below than 1meV/Å.

The analysis of the predicted evolutionary structure search gives -for MgZnO alloy- one candidate cubic Mg_3ZnO_4 phase, which belongs to the cubic space group *P*m3m. The optimized crystallographic parameters are given in Table I together with equilibrium structural properties for MgO and ZnO within the cubic (ZB and RS) and WZ phases.
To identify the miscibility of the alloy, we figure out the formation energy (ΔH), which describes the energy needed to form the alloys with respect to the binary constituents ZnO and MgO, defined as:

$$\Delta H = E(x) - (1-x)\, Ep(\mathrm{ZnO}) - x\, Ep(\mathrm{MgO})$$

Where $E(x)$ is the total energy of the alloy at composition x (x = 0.75 corresponding to Mg_3ZnO_4), and Ep(ZnO), Ep(MgO) represent the total energy of either (i) WZ (ZnO, and MgO), (ii) Cubic (RS CdO and MgO), (iii) Cubic (ZB CdO and MgO) and (iiii) RS (MgO)

and WZ(ZnO). We find $\Delta H_{WZ\text{-}WZ}$ = -0.189eV/paire, $\Delta H_{RS\text{-}RS}$ = -0.019eV/paire, $\Delta H_{ZB\text{-}ZB}$ = -0.239eV/paire and $\Delta H_{WZ\text{-}RS}$=0.035eV/paire. In the case of the end-point compounds have the same phase (case i-iii), ΔH is negative, hence the ordered phase Mg_3ZnO_4 is thermodynamically stable. Whereas, regarding ZnO and MgO having their ground state phases (i.e., case iiii), we found $\Delta H > 0$, which corresponds to phase separation into the binary WZ-ZnO and RS-MgO compounds. Nonetheless, the magnitude of $\Delta H_{WZ\text{-}RS}$ is once more, surprisingly very minor, advising that the ordered Mg_3ZnO_4 phase is only marginally instable. Besides we note the sequence of formation energies as $\Delta H_{WZ\text{-}RS} > \Delta H_{RS\text{-}RS} > \Delta H_{WZ\text{-}WZ} > \Delta H_{ZB\text{-}ZB}$. To gain better vision into these trends and to understand the physical factors at play, we separate ΔH [33], into two physically constituents, $\Delta H = \Delta E_{Chem} + \Delta E_{Ms}$ (1).

Here ΔE_{Chem} is the contribution to the total enthalpy, which describes chemical interactions (charge exchange, polarization…), whereas ΔE_{Ms} is a bulk microscopic strain emerged fundamentally from structural change in bond lengths and atomic relaxations. Fig. 2 reports the decomposition of Eq.1 for the four situations considered. We notice the following: (i) In the case where the end-point compounds have similar phase (i.e., cases i-iii), the relative strong negative value of the chemical piece (ΔE_{Chem}) leads to stability, nevertheless for the case iiii, ΔE_{Chem} is insufficient to stabilize the Mg_3ZnO_4 compound. (ii) ΔE_{Ms} and ΔE_{Chem} are rather strong (in absolute value) for the ZB-ZB and WZ-WZ cases, whereas these two components are rather weak for the RS-RS situation. The reason for these unlikeness can be assessed from the calculated Mg-O and Zn-O nearest-neighbor (NN) distances as function of alloy composition (Fig. 2): Whereas the first (1NN) and second (2NN) cation-anion bonds RS-ZnO and RS-MgO tend to remain nearly constant through the considered composition range. The ZB and WZ first and second-neighbor cation-anion distances Mg-O and Zn-O evidence distinguished dependence with composition. Accordingly, the bulk microscopic strain energy associated with the deformation of bond lengths is strong (weak) for the ZB-ZB, and WZ-WZ(RS-RS) cases.

Fig. 3 displays the charge transfer (CT) with a Löwdin charge analysis for the various phase of ZnO and MgO, where the RS-MgO and RS-ZnO are taken as a reference level for the CT. The charge transfer increases following the RS→ZB→WZ sequence. Note that the CT is enhanced for the WZ phase compared to the ZB one, as a consequence of the vanishing (presence) of spontaneous polarization (P_s) (see Table I) in the ZB (WZ) phase. Consequently, the chemical energy of formation, associated with charge exchange and/or

polarization is weak when MgO and ZnO adopt the fourfold-coordination (RS-phase), and strong when MgO and ZnO crystallize in the ZB or WZ phases.

The calculated elastic C_{ij} (Table I) of the ordered Mg_3ZnO_4 compound satisfy the mechanical restrictions, suggesting that the Mg_3ZnO_4 phase should be mechanically stable. In the calculated phonon band structure (Fig.4) and phonon density of states (PhDoS, Fig.5), no imaginary modes are detected in the whole Brillouin zone indicating the dynamical stability of the Mg_3ZnO_4 compound.

The calculated partial electronic density of states (PDoS) and band structure of Mg_3ZnO_4 are illustrated respectively in Fig.6 and Fig.7. The Zn-*d* and O-*p* electrons dominate the top of the valence bands from -8eV to Fermi-level, revealing bonding states via the well-known *p*-*d* coupling. The Zn-*d* states dominate between -8eV and -4eV (Zn(*d*)~95%, and O(*p*)~5%), whereas the valence band maximum (energy between -4eV and Fermi level) is contributed mainly by the *p*-states of oxygen.

We now examine the alloy band gap bowing, assuming a parabolic dependence; the composition dependent band gap $E_g(x)$ is described by the following equation:

$$E_g(x) = x\,E_g(\mathrm{MgO}) + (1-x)\,E_g(\mathrm{ZnO}) - b\,x\,(1-x).$$

Where $E_g(x)$ is the band gap of the alloy at composition $x = 0.75$, and $E_g(\mathrm{MgO})$, $E_g(\mathrm{ZnO})$ represents respectively the band-gap of MgO and ZnO, and b is the band gap bowing parameter. In order to get over the well-known DFT-band-gap 'disaster' (i.e., severe underestimation of excitation energies), we use the LDA-1/2 approach [34] to compute accurately the quasi-particle (QP) energies. At this level, the calculated QP band gaps for WZ-ZnO and RS-MgO are 3.51eV and 7.40eV respectively (Table I), in good agreement with experimental measurements (E_g(ZnO)~3.4eV[35], and E_g(MgO)~7.5eV[36]).

As a result of the mismatch in cation-oxygen coordination preferences (WZ vs. RS), the band-gap and band-gap bowing parameter *b* would exhibit marked end-point structure dependence. We therefore determine *b* for the different cases used in the calculation of the formation enthalpy. The calculated bowing parameter is given in Table II. Despite some obvious differences, both *b* values are strong, ranging from a downward-bowing ($b>0$, ~4.2eV) to an upward-bowing ($b<0$, ~-2.2eV). Among the four calculated optical band-gap bowing parameter and since the ordered alloy has the sixfold-coordinated phase, the most reliable result to take in mind, corresponds to the situation when the parent compounds (ZnO-MgO) and the ordered phase of the alloy have all the same coordination number (CN) (i.e., CN=6,

rocksalt-lattice), which corresponds to b~4.2eV. The latter bowing is in rough agreement with the calculated values of 3.1 eV [5] and 3.12eV [15].

To better understanding the physical content of the optical band gap bowing b, we follow Zunger and co-works [37], the origin of b is mainly related to two different physical effects, namly structural or geometric effect (b_{ST}). This results from the relative reponse of the binary compounds to hydrostatic pressure from their indivudual equilibrium volume to the alloy volume, and from the relaxation of the cation-anion bonds to their minum-energy configuration (see Refs. [38-50] for additional evidence). Finally, a chemical effect due to the redistribution of electron (charge exchange, b_{CE}). The calculate contributions (b_{ST}, b_{CE}) are given in Table II. We underline the following:

(i) The contribution due to structural effect is weak for the RS-RS case, since the small values of b_{ST} come from the relative weak band gap volume deformation potentials (BGDP) mismatch of RS-ZnO and RS-MgO (~9% [11]). However, the opposite hold for the WZ-WZ and ZB-ZB cases, since the large difference between BGDP of ZnO and MgO (~100% [11]) lead to the huge b_{ST}.

(ii) The chemical piece term b_{CE} is relatively large for all cases, b_{CE} scales with strong electronegativity mismatch of Mg and Zn atoms (($\Delta\chi/\chi$ ~ 23% using the Pauling's scale).

In summary, we have conducted a comprehensive study of energetic, mechanical, dynamical and electronic properties of ZnMgO alloys using first-principles calculations and evolutionary structure prediction. Our calculations revealed that the ordered Zn_3MgO_4 (space group Pm3m) is thermodynamically stable. Moreover this new structure is mechanically and dynamically stable as determined by checking the calculated elastic constants and phonon dispersions. Moreover, we found that the band gap bowing exhibit an appreciable end-point-parent structural dependence. Tacking account the coordination number of the ordered alloy, we obtain a strong optical band-gap bowing of ~4.2eV.

References

[1] A. Ohtomo, M. Kawasaki, T. Koida, K. Masubuchi, H. Koinuma, Y. Sakurai, Y. Yoshida, T. Yasuda, and Y. Segawa, Appl. Phys. Lett. **72**, 2466 (1998).

[2] J. Ishihara, A. Nakumura, S. Shigemori, T. Aoki, and J. Temmyo, Appl. Phys. Lett. **89**, 091914 (2006).

[3] S. Choopun, R. D. Vispute, W. Wang, R. P. Sharma, T. Venkatesan and H. Shen, Appl. Phys. Lett **80**, 1529 (2002).

[4] Y. –S. Kim, E. -C. Lee, and K. J. Chang, J. Korean Phys. Soc. **39**, 92 (2001).

[5] M. Sanati, G. L. W. Hart and A. Zunger, Phys. Rev. B **68**, 155210 (2003).

[6] A. Seko, F. Oba, A. Kuwabara and I. Tanaka, Phys. Rev. B **72**, 024107 (2005).

[7] R. Thangavel, M. Rajagopalan, and J. Kumar, Solid State Commun. **137**, 507 (2006).

[8] A. Malashevich and D. Vanderbilt, Phys. Rev. B **75**, 045106 (2007).

[9] X. F. Fan, H. D. Sun, Z. X. Shen, J. –L. Kuo and Y. M. Lu, J. Phys.: Condens. Matter **20**, 235221 (2008).

[10] X. Chen and J. Kang, Semicond. Sci. Technol. **23**, 025008 (2008).

[11] Y. Z. Zhu, G. D. Chen, H. Ye, A. Walsh, C. Y. Moon and S.-H. Wei, Phys. Rev. B **77**, 245209 (2008).

[12] X. D. Zhang, M. L. Guo, G. L. Liu, L. A. Zhang, W. Y. Zhang, Y. Q. Ding, Q. Wu, and X. Fen, Eur. Phys. J. B **62**, 417 (2008).

[13] I. V. Maznichenko, A. Ernst, M. Bouhassoune, J. Henk, M. Däne, L. Lüders, P. Bruno, W. Hergert, I. Mertig, Z. Szotek and W. M. Temmerman, Phys. Rev. B **80**, 144101 (2009).

[14] A. Schleife, M. Eisenacher, C. Rödel, F Fuchs, J. Furthmüller, and F. Bechstedt, Phys. Rev. B **81**, 245210 (2010).

[15] A. Schleife, C. Rödel, J. Furthmüller, and F. Bechstedt, New J. of Phys. **13**, 085012 (2011).

[16] K. Shimada, N. Takahashi, Y. Nakagawa, T. Hiramatsu, and H. Kato, Phys. Rev. B **88**, 075203 (2013).

[17] F. Tian, D. Duan, D. Li, C. Chen, X. Sha, Z. Zhao, B. Liu and T. Cui, Sci. Rep. **4**, 5759 (2014).

[18] J. Wang, Y. Tu, L. Yang, and H. Tolner, J. Comput. Electron **15**, 1521(2016).

[19] I Gorcyca, H Teisseyre, T Suski, N. E. Christensen, and A Savane, J. Appl. Phys. **120**, 215204 (2016).

[20] H. Yin, J. Chen, Y. Wang, J .Wang, and H. Guo, Sci. Rep. **7**, 41567 (2017).

[21] A. Zaoui and M. Ferhat, Solid State Commun. **151**, 867 (2011).

[22] E. Gregoryanz, C. Sanloup, M. Somayazulu, J. Badro, G. Fiquet, H. Mao, R. J. Hemley, Nat. Mater. **3**, 294 (2004)

[23] X. Zhang, G. Trimarchi, and A. Zunger, Phys. Rev. B **79**, 092102 (2009).

[24] W. Xie, Y. Xu, B. Liu, and D. G. Pettifor, Phys. Rev. Lett. **91**, 037204 (2003).

[25] A. Jain, S. P. Ong, G. Hautier, W. Chen, W. D. Richards, S. Dacek, S. Cholia, D. Gunter, D. Skinner, G. Ceder, and K. A. Persson, Apl. Mater. **1**, 011002 (2013), https://www.materialsproject.org

[26] G. Hautier, C. Fischer, V. Ehrlacher, A. Jain, and G. Ceder, Inorg. Chem. **50**, 656 (2011).

[27] W. Kohn and L. J. Sham, Phys. Rev. **140** A1133 (1965).

[28] P. Giannozzi et al., J. Phys. : Condens. Matter **21**, 395502 (2009).

[29] Y Wang and J P Perdew, Phys. Rev. B **43**, 8911 (1991).

[30] A. Dal Corso, Phys. Rev. B **82**, 075116 (2010) .

[31] H. J. Monkhorst and J. D. Pack, Phys. Rev. B 13, 5188 (1976) .

[32] S. Baroni, S. de Gironcoli, A. Dal Corso, and P. Giannozzi, Rev Mod. Phys. **73**, 515 (2001).

[33] G. P. Srivastava, J. L. Martins, and A. Zunger, Phys. Rev. B **31**, 2561 (1985).

[34] L. G. Ferreira, M. Marques, and L. K. Teles, Phys. Rev. B **78**, 125116 (2008).

[35] Current Topics in Materials Science **7**, edited by E. Kaldis (North Holland, Amsterdam, 1981), pp. 143-482.

[36] D. M. Roessler and W. C. Walker, phys. Rev. Lett. **17**, 310 (1966).

[37] J. E. Bernard and A. Zunger, Phys. Rev. B 36, 3199 (1987).

[38] A. Belabbes, A. Zaoui, S. Laref, M. Ferhat, Solid State Communications 152, 1700-1702 (2012).

[39] F. Boutaiba, A. Zaoui, M. Ferhat, Physica B 406, 265-269 (2011).

[40] A. Boukra, A. Zaoui and M. Ferhat, Journal of Applied Physics 108, 123904–123911(2010).

[41] H. Benaissa, A. Zaoui, M. Ferhat, Journal of Alloys and Compounds, 475, 592 – 594 (2009).

[42] H. Benaissa, A. Zaoui and M. Ferhat, Journal of Applied Physics 102, 113712-113717 (2007).

[43] S. Azzi, A. Zaoui and M. Ferhat, Solid State Communications 144, 245-248 (2007).

[44] A. Belabbes, A. Zaoui and M. Ferhat, Journal of Physics: Condensed Matter 19, 45621-45656 (2007).

[45] A. Berghout, A. Zaoui, J. Hugel, and M. Ferhat, Physical Review B75, 205112 - 205121(2007).

[46] A. Belabbes ,A. Zaoui and M. Ferhat, Materials Science and Engineer. B 137, 210-212 (2007).

[47] A. Belabbes , M. Ferhat and A. Zaoui, Applied Physics Letters 88, 152109-152112 (2006).

[48] A. Zaoui, Journal of Physics: Condensed Matter 14, 4025-4033(2002).

[49] M. Ferhat and A. Zaoui, Infrared Phys. and Tech. 42, 81-85 (2001).

[50] F. Tekia, M. Ferhat and A. Zaoui, Physica B 293, 183 (2000).

Table Captions

Table I: Calculated equilibrium structural parameters, elastic constants (GPa), first (1NN), and second (2NN) neighbor bond lengths distances (Å), spontaneous polarization P_{sp} (C/m^2) and band gaps (eV) for wurtzite (WZ), zinc-blende (ZB), and rocksalt (RS) MgO and ZnO compounds, and Zn_3MgO_4 compound.

Table II: Calculated band-gap bowing (eV) as well as its both contributions (b_{CT}, and b_{CE}).

Figure Captions

Fig. 1: Calculated total enthalpy ΔH, and the two contributions to ΔH (E_{Ms}, E_{Chem}) for the four considered cases: ZB-ZB, WZ-WZ, WZ-RS, and RS-RS.

Fig. 2: First (1NN) and second (2NN) nearest neighbor distances variation of ZB, RS, and WZ ZnO and MgO.

Fig. 3: Charge exchange variation of RS, ZB and WZ phases of ZnO and MgO.

Fig. 4: Phonon band structure of the ordered Mg_3ZnO_4 compound.

Fig. 5: Phonon density of states (PhDoS) of the ordered Mg_3ZnO_4 compound.

Fig. 6: Partial electronic density of states (PDoS) of the ordered Mg_3ZnO_4 compound.

Fig. 7: Electronic band structure of the ordered Mg_3ZnO_4 compound.

Table I

	WZ-ZnO	ZB-ZnO	RS-ZnO	WZ-MgO	ZB-MgO	RS-MgO	Mg_3ZnO_4
a(Å)	3.19	4.49	4.22	3.25	4.55	4.19	4.20
c/a	1.62			1.585			
u	0.376			0.378			
B	160.2	160.7	207.7	126.1	127.5	170.0	180.4
C_{11}	298.9	187.5	290.1	267.3	153.8	327.3	316.9
C_{12}	104.9	147.3	176.1	73.7	115.0	93.0	112.1
C_{13}	74.7			46.6			
C_{33}	342.0	187.4	290.1	283.9	153.8	327.3	316.9
C_{44}	59.9	134.6	89.0	68.2	134.5	147.9	132.1
δ(Zn-O)-1NN	1.9465	1.9449	2.1077				2.0990
δ(Mg-O)-1NN				1.9728	1.9715	2.0989	2.0990
δ(Zn-O)-2NN	3.7332	3.7243	3.6507				3.6354
δ(Mg-O)-2NN				3.8012	3.7752	3.6300	3.6354
P_{sp}	-0.04			-0.09			
E_g	3.51	3.41	4.88	6.26	6.23	7.40	5.95

Table II

	b_{ST}	b_{CE}	b
RS-RS	-0.11	4.32	4.21
WZ-RS	-0.49	2.97	2.48
WZ-WZ	-7.03	5.04	-2.00
ZB-ZB	-7.14	4.89	-2.25

Figure 1

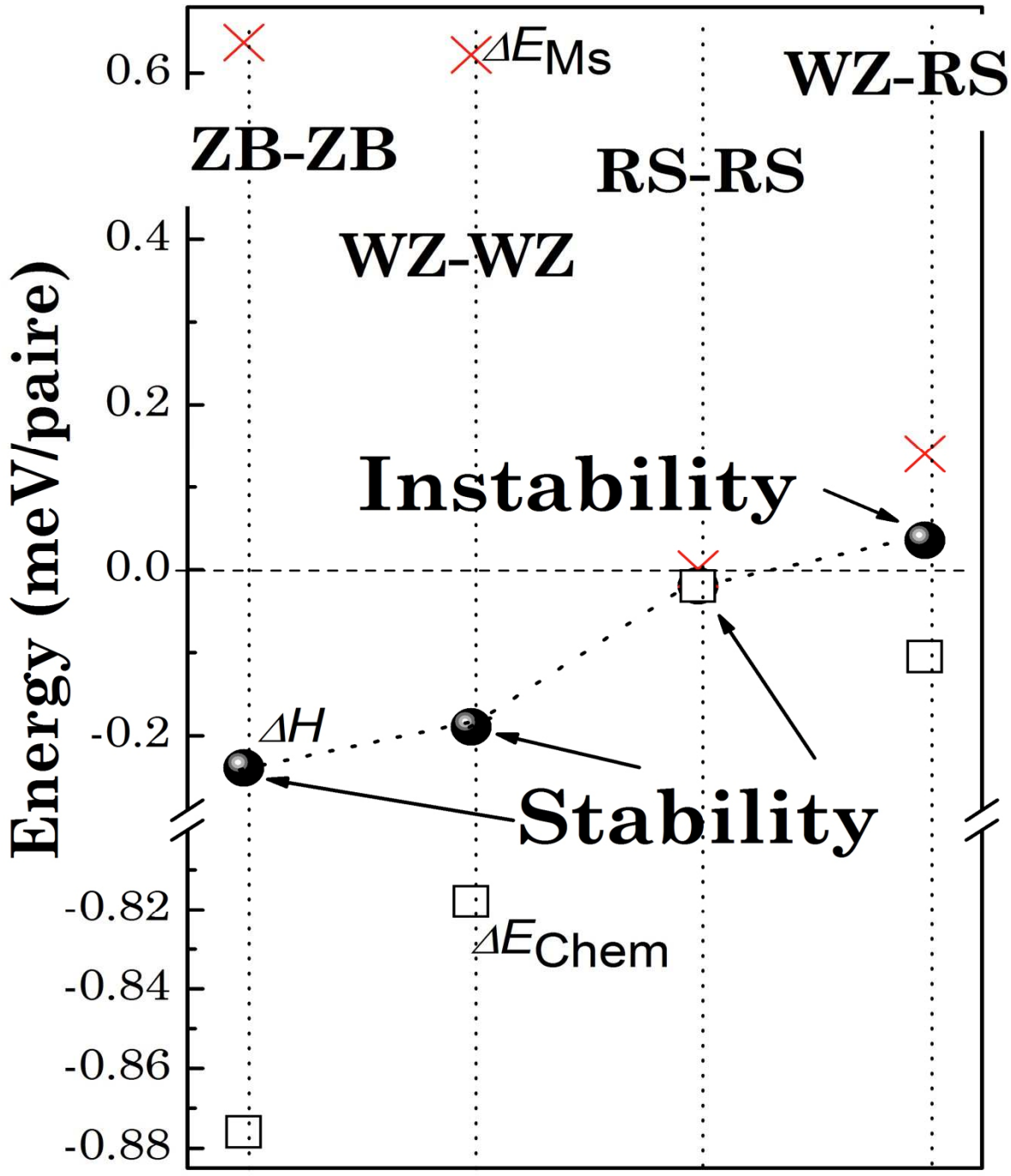
0.6
0.4
0.2
0.0
-0.2
-0.82
-0.84
-0.86
-0.88
Energy (meV/paire)
ΔEMs
WZ-RS
ZB-ZB
RS-RS
WZ-WZ
Instability
ΔH
Stability
ΔEChem

Figure 2

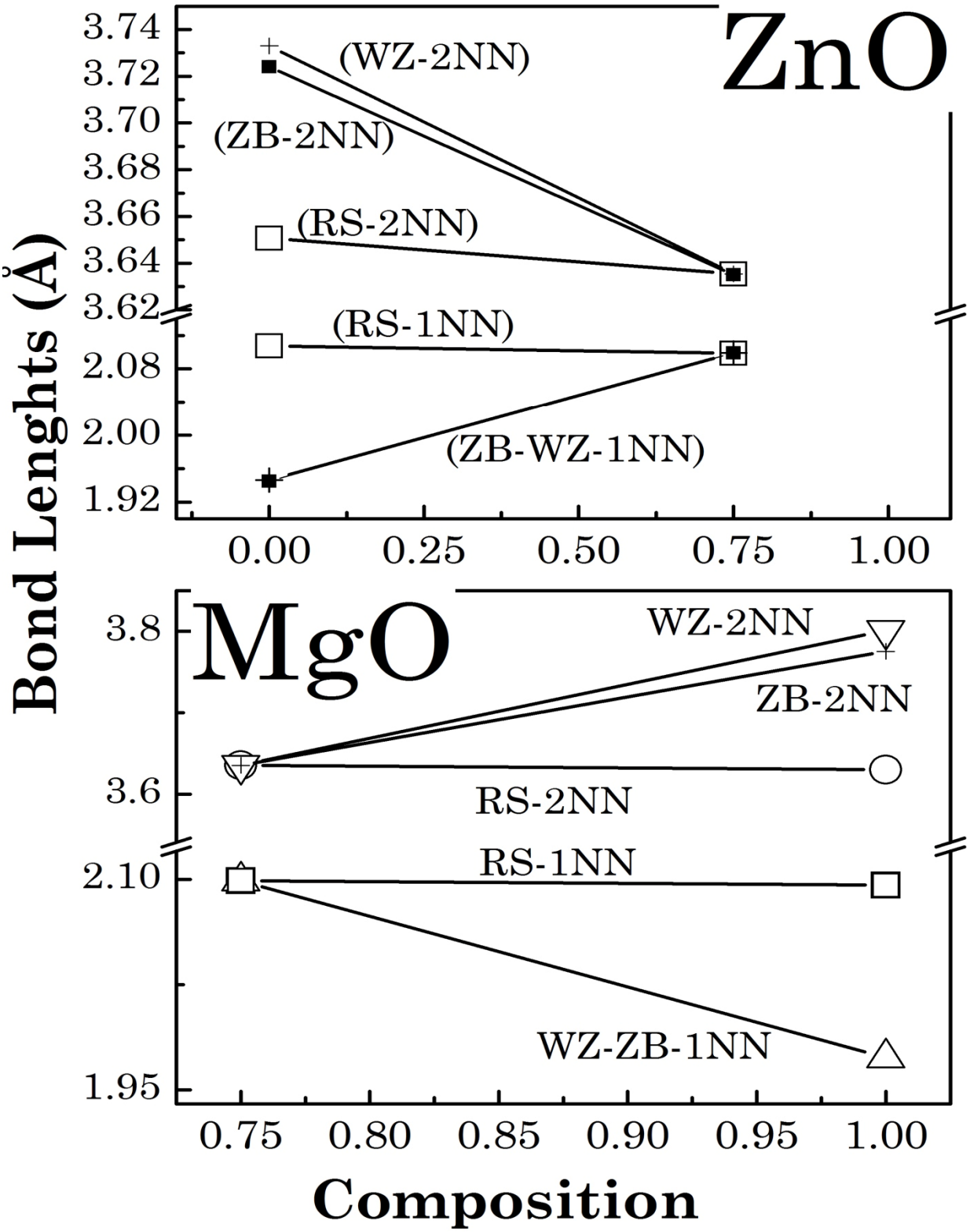
ZnO
(WZ-2NN)
(ZB-2NN)
(RS-2NN)
(RS-1NN)
(ZB-WZ-1NN)
3.74
3.72
3.70
3.68
3.66
3.64
3.62
2.08
2.00
1.92
0.00
0.25
0.50
0.75
1.00
MgO
WZ-2NN
ZB-2NN
RS-2NN
RS-1NN
WZ-ZB-1NN
3.8
3.6
2.10
1.95
0.75
0.80
0.85
0.90
0.95
1.00
Bond Lenghts (Å)
Composition

Fig. 3

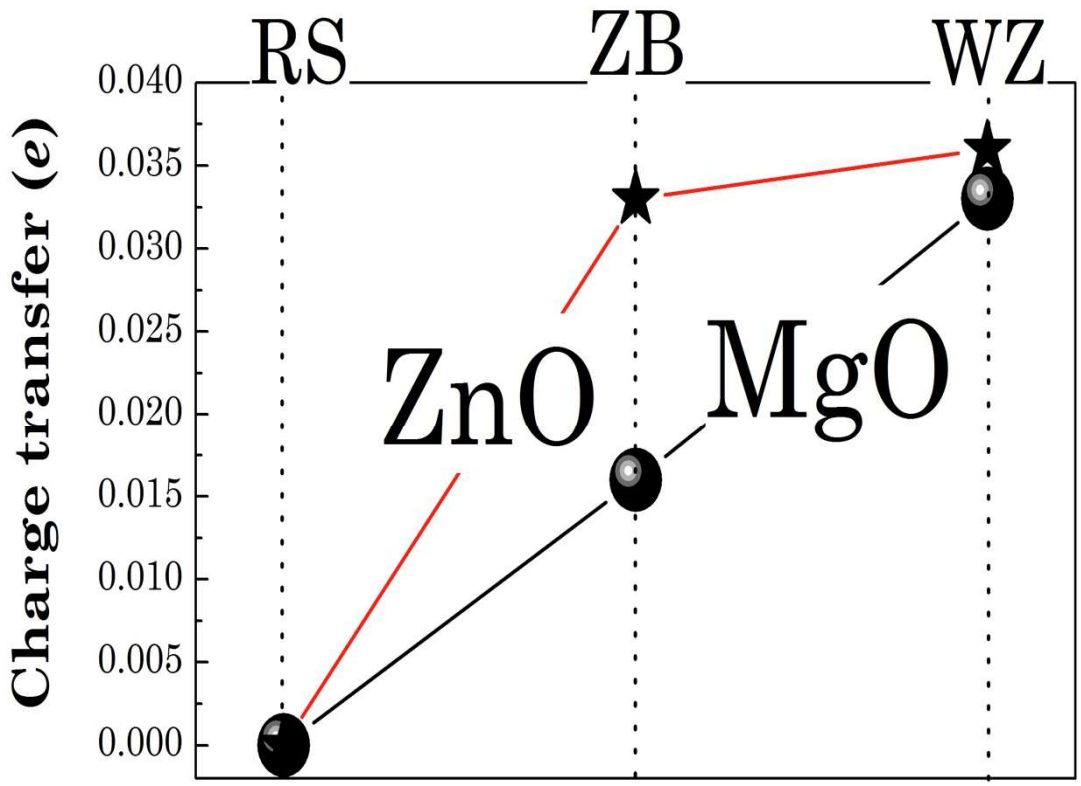
RS
ZB
WZ
0.040
0.035
0.030
0.025
0.020
0.015
0.010
0.005
0.000
Charge transfer (e)
ZnO
MgO

Fig. 4

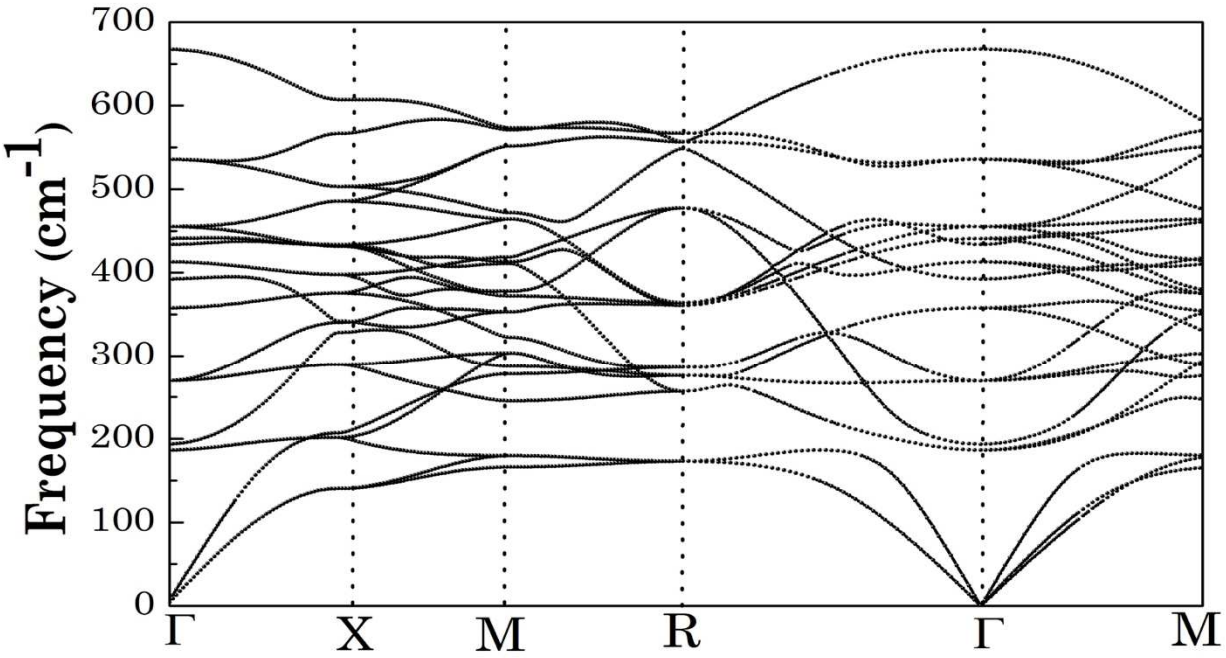

Fig. 5

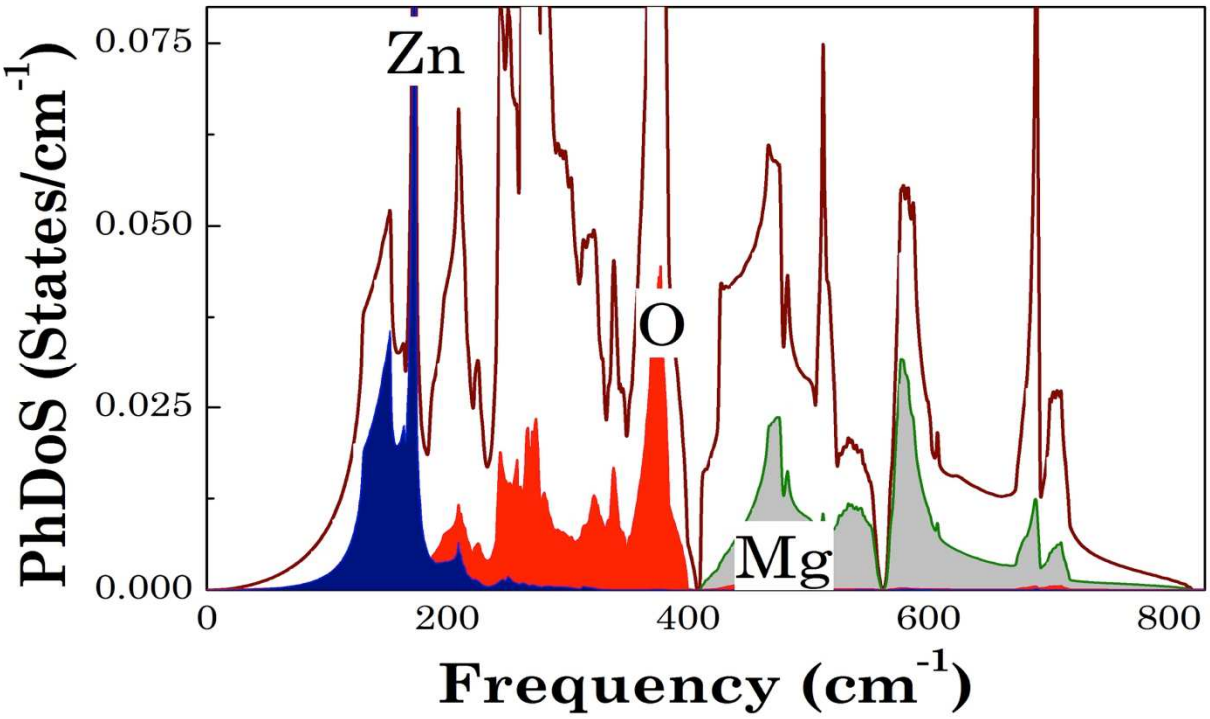
PhDoS (States/cm-1)
0.075
0.050
0.025
0.000
0
200
400
600
800
Frequency (cm-1)
Zn
O
Mg

Fig. 6

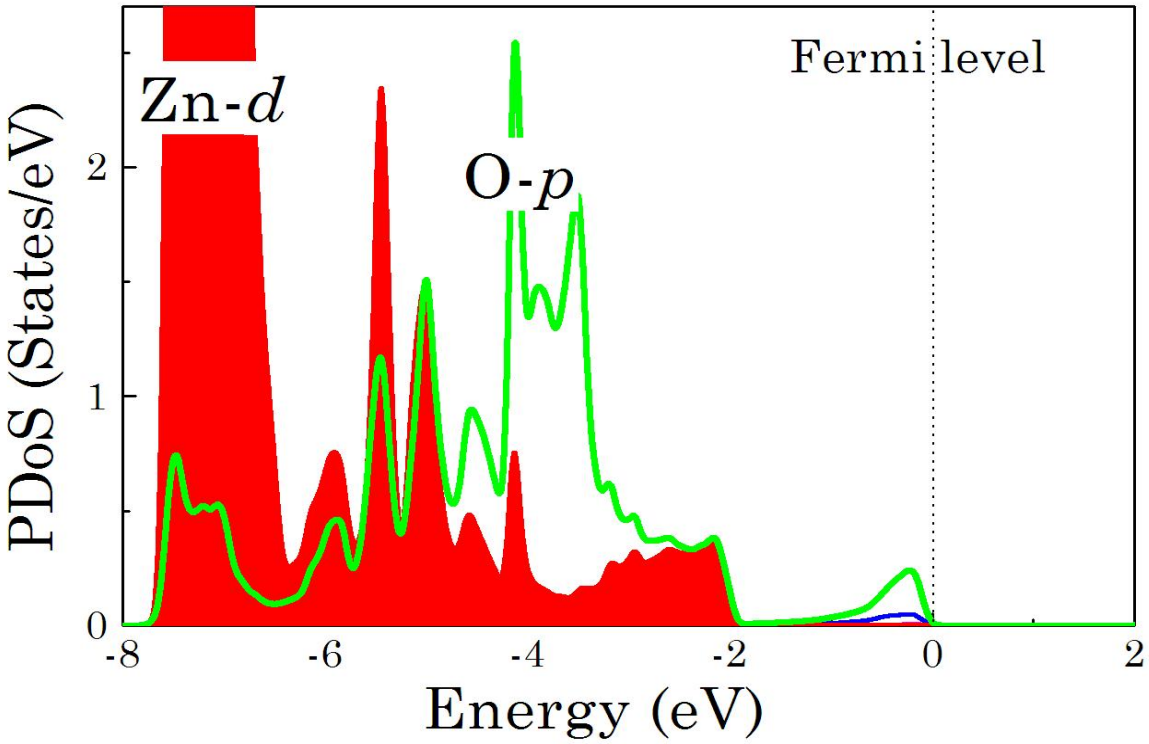

Fig. 7